

Characterization of the FAD-Containing *N*-Methyltryptophan Oxidase from *Escherichia coli*[†]

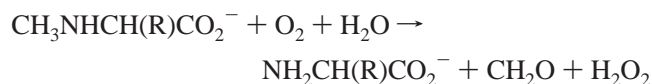
Peeyush Khanna and Marilyn Schuman Jorns*

Department of Biochemistry, MCP Hahnemann School of Medicine, Philadelphia, Pennsylvania 19129

Received October 20, 2000

ABSTRACT: *N*-Methyltryptophan oxidase (MTOX) is a flavoenzyme that catalyzes the oxidative demethylation of *N*-methyl-L-tryptophan and other *N*-methyl amino acids, including sarcosine, which is a poor substrate. The *Escherichia coli* gene encoding MTOX (*solA*) was isolated on the basis of its sequence homology with monomeric sarcosine oxidase, a sarcosine-inducible enzyme found in many bacteria. These studies show that MTOX is expressed as a constitutive enzyme in a wild-type *E. coli* K-12 strain, providing the first evidence that *solA* is a functional gene. MTOX expression is enhanced 3-fold by growth on minimal media but not induced by *N*-methyl-L-tryptophan, L-tryptophan, or 3-indoleacrylate. MTOX forms an anionic flavin semiquinone and a reversible, covalent flavin–sulfite complex ($K_d = 1.7$ mM), properties characteristic of flavoprotein oxidases. Rates of formation ($k_{on} = 5.4 \times 10^{-3} \text{ M}^{-1} \text{ s}^{-1}$) and dissociation ($k_{off} = 1.3 \times 10^{-5} \text{ s}^{-1}$) of the MTOX–sulfite complex are orders of magnitude slower than observed with most other flavoprotein oxidases. The pK_a for ionization of oxidized FAD at N(3)H in MTOX (8.36) is two pH units lower than that observed for free FAD. The MTOX active site was probed by characterization of various substrate analogues that act as competitive inhibitors with respect to *N*-methyl-L-tryptophan. Qualitatively similar perturbations of the MTOX visible absorption spectrum are observed for complexes formed with various aromatic carboxylates, including benzoate, 3-indole-(CH₂)_{*n*}-CO₂[−] and 2-indole-CO₂[−]. The most stable complex with 3-indole-(CH₂)_{*n*}-CO₂[−] is formed with 3-indolepropionate ($K_d = 0.79$ mM), a derivative with the same side chain length as *N*-methyl-L-tryptophan. Benzoate binding is enhanced upon protonation of a group in the enzyme–benzoate complex ($pK_{EL} = 6.87$) but blocked by ionization of a group in the free enzyme ($pK_E = 8.41$), which is attributed to N(3)H of FAD. Difference spectra observed for the aromatic carboxylate complexes are virtually mirror images of those observed with sarcosine analogues (*N,N'*-dimethylglycine, *N*-benzylglycine). Charge-transfer complexes are formed with 3-indoleacrylate, pyrrole-2-carboxylate, and CH₃XCH₂CO₂[−] (X = S, Se, Te).

N-Methyltryptophan oxidase (MTOX)¹ catalyzes the oxidative demethylation of various *N*-methyl amino acids, generating the unsubstituted amino acid, formaldehyde and hydrogen peroxide. The enzyme exhibits a preference for



amino acids with aromatic or large aliphatic side chains. *N*-Methyltryptophan is currently the best known substrate. Sarcosine (*N*-methylglycine), the simplest *N*-methyl amino acid, is a poor substrate for MTOX (1, 2). The gene encoding MTOX (*solA*) was, however, isolated from a wild-type strain of *Escherichia coli* K-12 (W3110) on the basis of its sequence homology with monomeric sarcosine oxidase (MSOX) (1). MSOX is a sarcosine-inducible bacterial enzyme that is important in the catabolism of sarcosine, a

common soil metabolite that can act as sole source of carbon and energy for many microorganisms (3). Unlike sarcosine, the preferred substrates of MTOX are not common metabolites, although *N*-methyltryptophan has been identified in several plant species (4) and *N*-methyl amino acids are found in polyketide antibiotics (5). The metabolic role(s) of MTOX in *E. coli* and its physiological substrate are unknown. Nevertheless, it should be noted that MTOX is considerably more efficient in oxidizing *N*-methyl-L-tryptophan ($k_{cat}/K_m = 1.24 \times 10^7 \text{ M}^{-1} \text{ min}^{-1}$) (2) than is MSOX in oxidizing sarcosine ($k_{cat}/K_m = 7.5 \times 10^5 \text{ M}^{-1} \text{ min}^{-1}$) (6).

MTOX is a monomeric flavoenzyme (42 kDa) and contains FAD [8α-(*S*-cysteinyl)FAD] covalently linked to a cysteine residue (7). MTOX is a member of a recently recognized flavoprotein family of eukaryotic and prokaryotic amine oxidases that includes MSOX, pipecolate oxidase, and heterotetrameric sarcosine oxidase (7–9). The crystal structures of MSOX and its complexes with substrate analogues has recently been determined (10, 11). MTOX shares 43% sequence identity with MSOX. More than a dozen residues at or near the active site of MSOX are conserved in MTOX. The structural basis for the large difference in substrate specificity of the two enzymes remains to be determined.

[†] This work was supported in part by Grant GM 31704 from the National Institutes of Health.

* To whom correspondence should be addressed. Phone: (215) 991-8580. FAX: (215) 843-8849. E-mail: marilyn.jorns@drexel.edu.

¹ Abbreviations: MTOX, *N*-methyltryptophan oxidase; MSOX, monomeric sarcosine oxidase; FAD, flavin adenine dinucleotide; EDTA, ethylenediaminetetraacetic acid.

This paper focuses on characterizing the amino acid substrate binding site and the properties of the prosthetic group in recombinant MTOX. We also report expression of the *solA* gene in *E. coli* W3110 under various growth conditions.

EXPERIMENTAL PROCEDURES

Materials. Glucose oxidase (*Aspergillus niger*, Type V-S) benzoic acid, *N,N'*-dimethylglycine, methyl viologen, horseradish peroxidase, *o*-dianisidine, anthranilic acid, DL-3-indoleacetic acid, *N*-methyltryptophan, and pyrrole-2-carboxylic acid were purchased from Sigma. Sarcosine, 2-indolecarboxylic acid, 3-indolecarboxylic acid, 3-indolepropionic acid, 3-indolebutyric acid, DL-3-indolelactic acid, *trans*-3-indoleacrylic acid, *N*-benzylglycine, and methylthioacetic acid were obtained from Aldrich. Sodium sulfite was from Fluka. 5-Deazariboflavin was synthesized as previously described (12). The potassium salts of methylselenoacetate (MSEA) and methyltelluroacetate (MTEA) were generous gifts from Dr. Louis Silks [National Stable Isotope Resource at Los Alamos and NIH Supported Resource (RR02231)]. *E. coli* W3110 (CGSC#4474) was obtained from the *E. coli* Genetic Stock Center.

Expression of MTOX in *E. coli*. *E. coli* W3110 cells were grown at 37 °C in various media, including LB (13), tryptone-phosphate (14), Vogel-Bonner (15), and a modified Clark and Maaloe medium as described by Jensen (16). In some experiments, the media contained compounds added as possible inducers of MTOX expression, as indicated. The harvested cells were sonicated and subjected to a stepwise ammonium sulfate fractionation (0–50%, 50–75% or 0–40%, 40–75%), similar to that previously described for recombinant MTOX (7). After dialysis of the fractions versus 50 mM potassium phosphate buffer, pH 8.0, containing 1 mM EDTA, MTOX activity and protein assays were performed, as described by Wagner et al. (7). With most extracts, >75% of MTOX activity was recovered in the 50–75% or 40–75% fraction, similar to that observed with recombinant enzyme. Reported specific activities are the weighted average of values observed for the two ammonium sulfate fractions.

Purification and Assay of Recombinant MTOX. *E. coli* strain JM109/pESOX1 was grown at 37 °C in LB media containing carbenicillin as previously described (7). Enzyme purification, routine protein, and activity assays were performed as described by Wagner et al. (7). A horseradish peroxidase-coupled assay, similar to that described by Wagner and Jorns (6), was used to investigate the effect of various ligands on MTOX activity. Reactions were conducted in 100 mM potassium phosphate buffer, pH 8.0, containing 1 mM EDTA at 25 °C.

Spectroscopy. Absorption spectra were recorded using a Perkin-Elmer Lambda 2S spectrometer. Anaerobic experiments were conducted as previously described (11). The concentration of MTOX was determined using the previously determined extinction coefficient for oxidized enzyme at 457 nm ($\epsilon_{457} = 13\,300\text{ M}^{-1}\text{ cm}^{-1}$ at pH 8.0) (7). An extinction coefficient for the anionic flavin radical ($\epsilon_{393} = 28\,800\text{ M}^{-1}\text{ cm}^{-1}$) was determined after quantitative conversion of the oxidized enzyme to the radical form by 5-deazariboflavin-mediated photoreduction in the presence of methyl viologen at pH 8.0. Photoreduction experiments were conducted by

irradiating the anaerobic sample with two 15 W blue-black fluorescent tubes (Sylvania F15T8BLB).

Spectral titrations with active site ligands were conducted at 4 °C in 50 mM potassium phosphate buffer, pH 8.0, containing 1 mM EDTA, unless otherwise noted. [For selected ligands, dissociation constants were also determined under the same conditions used for steady-state kinetic studies (25 °C, 100 mM potassium phosphate buffer, pH 8.0, containing 1 mM EDTA).] All spectra are corrected for dilution. For comparison of the spectral perturbations observed with different ligands (see Figures 5–8), difference and absolute spectra were normalized to the same initial concentration of uncomplexed MTOX ($A_{457} = 0.5$). (The observed initial A_{457} varied from about 0.45 to 0.6 in different experiments.) Spectra were also normalized to 100% complex formation to compensate for differences in the maximal extent of complex formation observed in titrations with different ligands. The 100% complex spectra were calculated using the measured complex dissociation constants and spectral data obtained at the highest ligand concentration tested. Difference spectra were used to determine the position of charge-transfer bands in the case of ligands (methylthioacetate, pyrrole-2-carboxylate) where the bands overlapped with the red edge of the flavin absorption spectrum.

Data Analysis. Data were fit to eqs 1–4 using the curve fit function in Sigma Plot (Jandel Corporation). Equation 1 was used to fit the effect of pH on the absorption spectrum of MTOX. Y is the observed absorbance at 395 nm at a given pH value. A and B are the calculated absorbance at 395 nm at low and high pH values, respectively. Equation 2 was used for analysis of spectrophotometric titration data for complex formation between MTOX and various ligands.

$$Y = \frac{AH^+ + BK_a}{H^+ + K_a} \quad (1)$$

$$Y = \frac{AX}{X + K} \quad (2)$$

$$Y = Ae^{-kt} + B \quad (3)$$

Y and A are the observed and maximal absorbance change at the wavelength selected for analysis, respectively, X is the concentration of the varied ligand, and K is the complex dissociation constant. Equation 3 was used to fit first-order reaction kinetics. Y is the observed absorbance at the selected wavelength and time = t , A is the maximal absorbance change, and B is the final absorbance at the selected wavelength. Equation 4 is described in Results.

RESULTS

Expression of MTOX in a Wild-Type *E. coli* K-12 Strain. Recombinant MTOX constitutes about 30% of the protein in crude cell extracts when expression of the *solA* gene is placed under the control of the *lacUV5* promoter (7). It was not, however, known whether *solA* is a functional gene in wild-type strains of *E. coli* since MTOX activity had never been measured in such strains. We grew a wild-type *E. coli* K-12 strain (W3110) on various media, including a modified Clark and Maaloe medium (16), Vogel-Bonner (15), LB, and tryptone-phosphate (14). MTOX activity was measured after

Table 1: Expression of MTOX in *E. coli* W3110 Cells Grown in Various Media

growth medium ^b	specific activity (nmol min ⁻¹ mg ⁻¹) ^a
Clark and Maaloe	
none	3.2 ± 0.9
plus <i>N</i> -methyl-L-tryptophan	4.1 ± 0.6
plus 3-indoleacrylate	2.6 ± 0.5
plus L-tryptophan	2.7 ± 0.7
Vogel-Bonner	4.5 ± 0.8
LB	1.3 ± 0.5
tryptone-phosphate	1.1 ± 0.2

^a MTOX activity was measured after ammonium sulfate fractionation of crude cell extracts, as detailed in the methods section. ^b Media contained 5–10 mM (*N*-methyl)-L-tryptophan or 80 μ M indoleacrylate, where indicated.

ammonium sulfate fractionation of crude cell extracts. MTOX activity was detected in all extracts, but expression levels were about 3-fold higher when the wild-type strain was grown on minimal media (Vogel-Bonner, modified Clark and Maaloe) as compared with rich media (LB, tryptone-phosphate) (Table 1).

MTOX constitutes about 0.01% of the protein in the ammonium sulfate fraction from cells grown on modified Clark and Maaloe medium, as judged by comparison with the specific activity reported for pure, recombinant MTOX (36.2 U/mg) (7). Bacterial sarcosine oxidases may constitute a few percent of the protein in crude extracts from cells grown in the presence of sarcosine which induces expression of these enzymes (17). Induction of *solA* expression was not, however, observed when cells were grown on modified Clark and Maaloe medium in the presence of *N*-methyl-L-tryptophan, the best known substrate for MTOX (Table 1). Indoleacrylate, an antirepressor of the *trp* repressor, induces expression of genes related to tryptophan biosynthesis that are under the control of the *trp* promoter (18, 19). The compound does not, however, induce expression of the *solA* gene when added to the modified Clark and Maaloe medium (Table 1). L-Tryptophan also did not affect MTOX expression.

Anaerobic Photoreduction and Reaction of Recombinant MTOX with Sulfite. Formation of a reversible, covalent flavin–sulfite adduct and a red, anionic flavin radical are properties that generally distinguish oxidases from other classes of flavoproteins (20, 21). MTOX forms a red, anionic radical upon anaerobic photoreduction mediated by 5-deazariboflavin (22), as judged by the development of an intense new absorption band at 393 nm ($\epsilon_{393} = 28\,800\text{ M}^{-1}\text{ cm}^{-1}$), accompanied by the bleaching of the 457 nm band of the oxidized enzyme (Figure 1). Reduction of the radical to 1,5-dihydroFAD occurred upon further illumination (Figure 1, inset). The observed spectral changes were fully reversed upon aeration.

Since preliminary studies indicated that MTOX reactivity with sulfite was enhanced at lower pH values, these reactions were conducted at the lowest value (pH 6.0) compatible with MTOX long-term stability. As judged by the characteristic bleaching of the flavin absorption spectrum (Figure 2, panel A), MTOX does form a typical covalent flavin–sulfite complex in a reaction that exhibits apparent first-order kinetics (Figure 2, panel B, curves 1–5). The MTOX complex is moderately stable ($K_d = 1.7\text{ mM}$), but complex

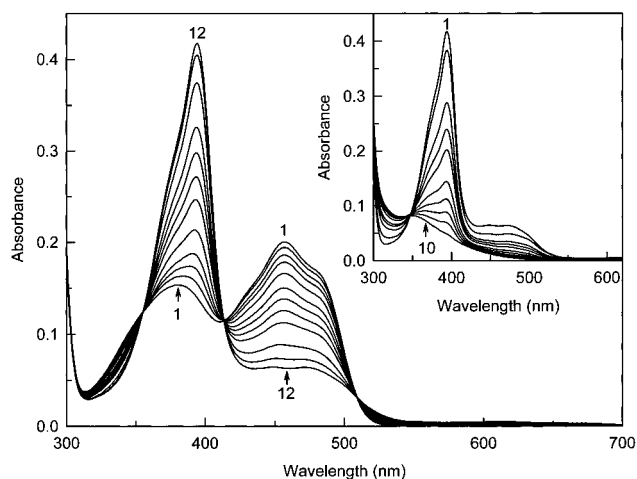


FIGURE 1: Anaerobic photoreduction of MTOX. Curve 1 shows the absorption spectrum of the oxidized enzyme (15.3 μ M) in 50 mM potassium phosphate buffer, pH 8.0, containing 8 mM EDTA, 0.25 μ M 5-deazariboflavin, and 25 μ M methyl viologen. Curves 2–12 were recorded after illumination at room temperature for 20, 40, 60, 100, 150, 200, 250, 300, 400, 500, and 580 s, respectively. Inset: The spectrum obtained after 580 s or 9.7 min of illumination is shown in curve 1. Curves 2–10 were recorded after illumination for 14, 16, 18, 20, 22, 24, 26, 28, and 32 min, respectively.

formation is extremely slow and required days to reach equilibrium, even at pH 6.0. A plot of k_{obs} versus sulfite concentration was linear ($r^2 = 0.999$, plot not shown). Values for the rate of complex formation ($k_{\text{on}} = 5.4 \times 10^{-3}\text{ M}^{-1}\text{ s}^{-1}$) and dissociation ($k_{\text{off}} = 1.3 \times 10^{-5}\text{ s}^{-1}$) were obtained from the slope and y-intercept, respectively. The K_d value calculated for the MTOX complex based on the observed rate constants ($K_d = k_{\text{off}}/k_{\text{on}} = 2.4\text{ mM}$) is in fairly good agreement with that determined from titration results ($K_d = 1.7\text{ mM}$). The reversibility of the sulfite reaction with MTOX is demonstrated by the time-dependent recovery of flavin absorbance upon mixing the sulfite complex with excess 3-indolepropionate (Figure 2, panel B, curve 6), an active site ligand that rapidly binds to uncomplexed MTOX (vide infra). The rate of sulfite complex dissociation observed upon adding 3-indolepropionate ($k = 1.6 \times 10^{-5}\text{ s}^{-1}$) is in good agreement with the value obtained for k_{off} ($1.3 \times 10^{-5}\text{ s}^{-1}$).

Effect of pH on the Absorption Spectrum. Recombinant MTOX exhibits absorption maxima at 457 and 382 nm at pH 7.14. As the pH is increased to 10.03, the 382 nm peak undergoes a pronounced hypsochromic shift to 367 nm, accompanied by a decrease in absorbance at 457 nm (Figure 3). The spectral changes resemble those observed with free FAD upon ionization at the N(3)H position (23). A pK_a value of 8.36 for the MTOX flavin was obtained by fitting the absorbance change at 395 nm to a theoretical pH-titration curve (Figure 3, inset). The pK_a observed with MTOX is shifted downward by two pH units as compared with free flavin ($pK_a = 10.4$) (23).

Identification of Active Site Ligands. A variety of aromatic and aliphatic carboxylates bind to the active site of recombinant MTOX (Tables 2 and 3). These ligands were identified based on their ability to perturb the flavin absorption spectrum, as illustrated by the results obtained with benzoate (Figure 4). The wavelength of maximal absorbance change (494 nm) was determined from difference spectra recorded during the titration (Figure 4, panel A). The complex dissociation constant ($K_d = 37.2\text{ mM}$) was determined by

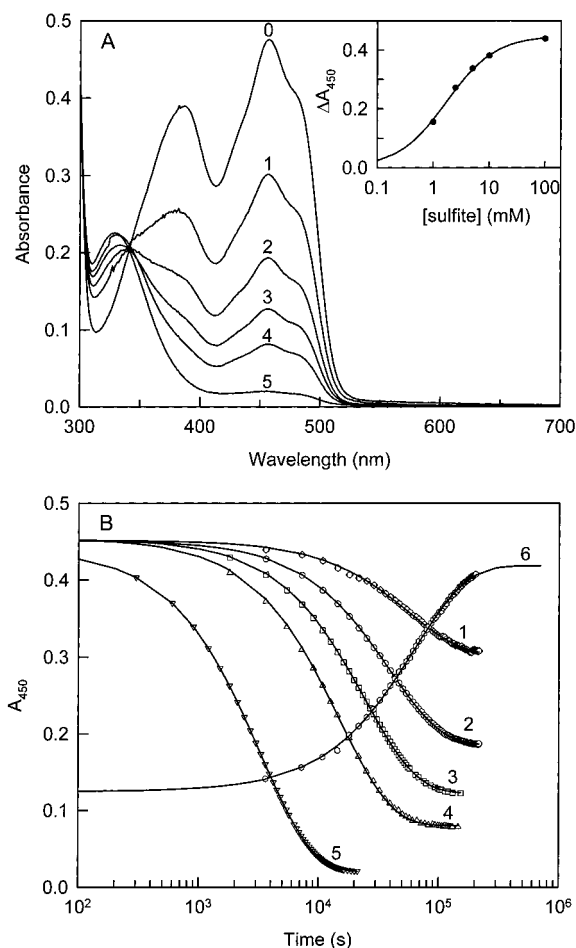


FIGURE 2: Reaction of MTOX with sulfite. Panel A: Curve 0 is the absorption spectrum of a dilution of MTOX into 50 mM potassium phosphate buffer, pH 6.0, containing 1 mM EDTA at 4 °C in the absence of sulfite. Identical dilutions were made into the same buffer containing 1, 2.5, 5, 10, or 100 mM sulfite and spectra (curves 1 to 5, respectively) were recorded 60, 60, 42.5, 40.5, and 5.9 h, respectively, after mixing. The inset shows a plot of the change in absorbance at 450 nm as a function of the sulfite concentration. The solid line is a fit of the data to a theoretical binding curve. Panel B: Curves 1 to 5 show the time course of the absorbance decrease at 450 nm observed upon mixing MTOX with 1, 2.5, 5, 10, and 100 mM sulfite, respectively. Curve 6 shows the time course of the dissociation of the sulfite complex (formed with 5 mM sulfite) observed upon addition of 10 mM 3-indolepropionate. The solid lines are a fit of the data to a single exponential expression.

fitting absorbance changes at 494 nm to a theoretical binding curve (Figure 4, panel B). Absolute spectra show that benzoate causes hypsochromic shifts of the 457 and 382 nm bands of free MTOX to 449 and 378 nm, respectively, accompanied by an increase in extinction (Figure 4, panel C).

Steady-state kinetic studies with benzoate and *N*-benzylglycine indicate that the compounds are competitive inhibitors with respect to *N*-methyltryptophan. The observed inhibition constants at 25 °C ($K_i = 23.2$ and 6.1 mM, respectively) are in moderately good agreement with the complex dissociation constants as determined by spectral titration under the same conditions ($K_d = 38.1$ and 8.7 mM, respectively).

Indole and Other Aromatic Carboxylate Ligands. The binding affinity of MTOX for 3-substituted indole carboxy-

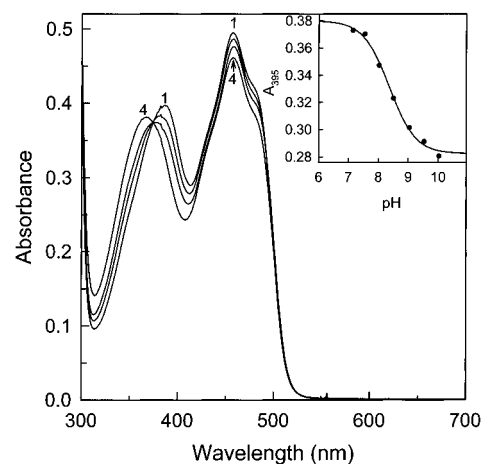
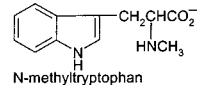
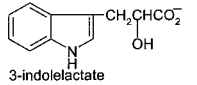
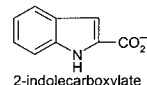
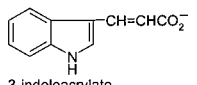
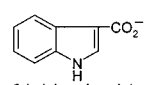
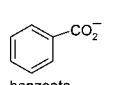
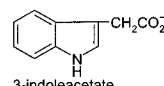
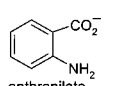
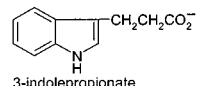
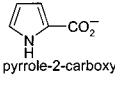
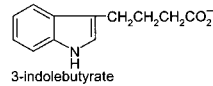


FIGURE 3: Effect of pH on the absorption spectrum of MTOX. Curves 1–4 were recorded at 4 °C in 50 mM potassium phosphate buffer containing 1 mM EDTA at pH 7.14, 8.02, 8.50, and 10.03, respectively. The inset shows a plot of MTOX absorbance at 395 nm as a function of pH. The curve shows a fit of the data points (solid circles) to a theoretical pH-titration curve.

Table 2: Indole and Other Aromatic Carboxylates as Ligands for MTOX¹

Compound	K_d (mM)	Compound	K_d (mM)
 N-methyltryptophan	0.37 ²	 3-indolelactate	0.28
 2-indolecarboxylate	18.3	 3-indoleacrylate	5.5 (CT complex)
 3-indolecarboxylate	115	 benzoate	37.2 (38.1) ³
 3-indoleacetate	6.9	 anthranilate	11.8 (CT complex)
 3-indolepropionate	0.79	 pyrrole-2-carboxylate	25.1 (CT complex)
 3-indolebutyrate	1.3		

¹ Unless otherwise indicated, dissociation constants were determined by spectral titration at 4 °C. ² K_m determined in steady-state kinetic studies at 25 °C (2). ³ The dissociation constant was determined by spectral titration at 25 °C.

lates is dependent on the number of methylene groups between the ring and the carboxyl group [3-indole-(CH₂)_n-CO₂⁻]. An increase in binding affinity is observed as *n* is increased from 0 to 2. In this range, an excellent linear

Table 3: Sarcosine Analogues as Ligands for MTOX¹

Compound	K _d (mM)	Compound	K _d (mM)
$\begin{array}{c} \text{CH}_2\text{CO}_2^- \\ \\ \text{HNCH}_3 \\ \text{sarcosine} \end{array}$	39 ²	$\begin{array}{c} \text{CH}_2\text{CO}_2^- \\ \\ \text{SCH}_3 \\ \text{methylthioacetate} \end{array}$	32.3 (CT complex)
$\begin{array}{c} \text{CH}_2\text{CO}_2^- \\ \\ \text{HNCH}_2 \\ \\ \text{C}_6\text{H}_5 \\ \text{N-benzylglycine} \end{array}$	7.8 (8.7) ³	$\begin{array}{c} \text{CH}_2\text{CO}_2^- \\ \\ \text{SeCH}_3 \\ \text{methylselenoacetate} \end{array}$	4.8 (CT complex)
$\begin{array}{c} \text{CH}_2\text{CO}_2^- \\ \\ \text{CH}_3\text{NCH}_3 \\ \text{dimethylglycine} \end{array}$	32.4 (49.9) ³	$\begin{array}{c} \text{CH}_2\text{CO}_2^- \\ \\ \text{TeCH}_3 \\ \text{methyltelluroacetate} \end{array}$	6.6 (CT complex)

¹ Unless otherwise indicated, dissociation constants were determined by spectral titration at 4 °C. ² Determined from anaerobic half-reaction kinetics studies at 4 °C (2). ³ The dissociation constant was determined by spectral titration at 25 °C.

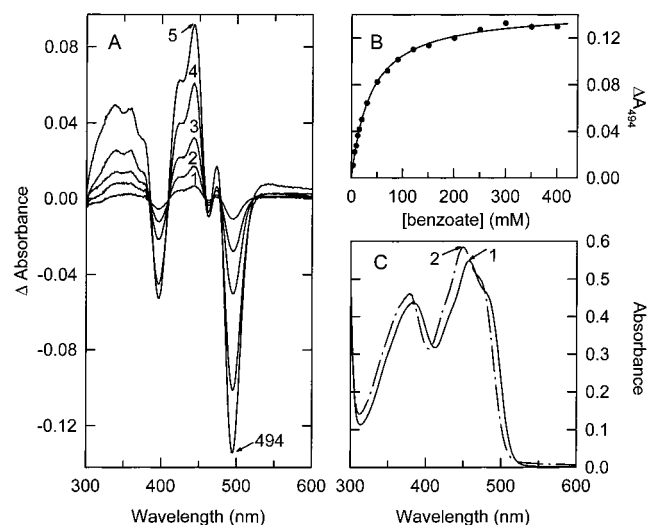


FIGURE 4: Titration of MTOX with benzoate. Panel A: Curves 1–5 are difference spectra recorded after adding 3, 9, 20, 90, and 500 mM benzoate, respectively, to 41.2 μ M MTOX. Panel B: The observed decrease in absorbance at 494 nm (solid circles) is plotted as a function of the benzoate concentration. The solid line is a fit of the data to a theoretical binding curve ($K_d = 37.2$ mM). Panel C: Curves 1 and 2 are absolute spectra recorded after adding 0 and 500 mM benzoate, respectively. The latter spectrum represents 93.3% complex formation, as estimated based on the observed K_d value.

correlation ($r^2 = 0.994$, slope = 1370 cal/mol, y-intercept = -1250 cal/mol) is found between binding energy and n (Figure 5, panel E). When n is increased from 2 to 3, a small decrease in binding energy is observed (0.28 kcal), suggesting a steric restriction on the length of the side chain that can be accommodated at the active site.

It is noteworthy that the tightest binding with 3-substituted indole carboxylates is observed with 3-indolepropionate (3-indole-(CH₂)₂-CO₂⁻ $K_d = 0.79$ mM), a derivative where the side chain length is the same as the best known substrate, *N*-methyltryptophan. Introduction of a double bond into the 3-indolepropionate side chain results in a 7-fold decrease in binding affinity, as judged by results obtained with 3-in-

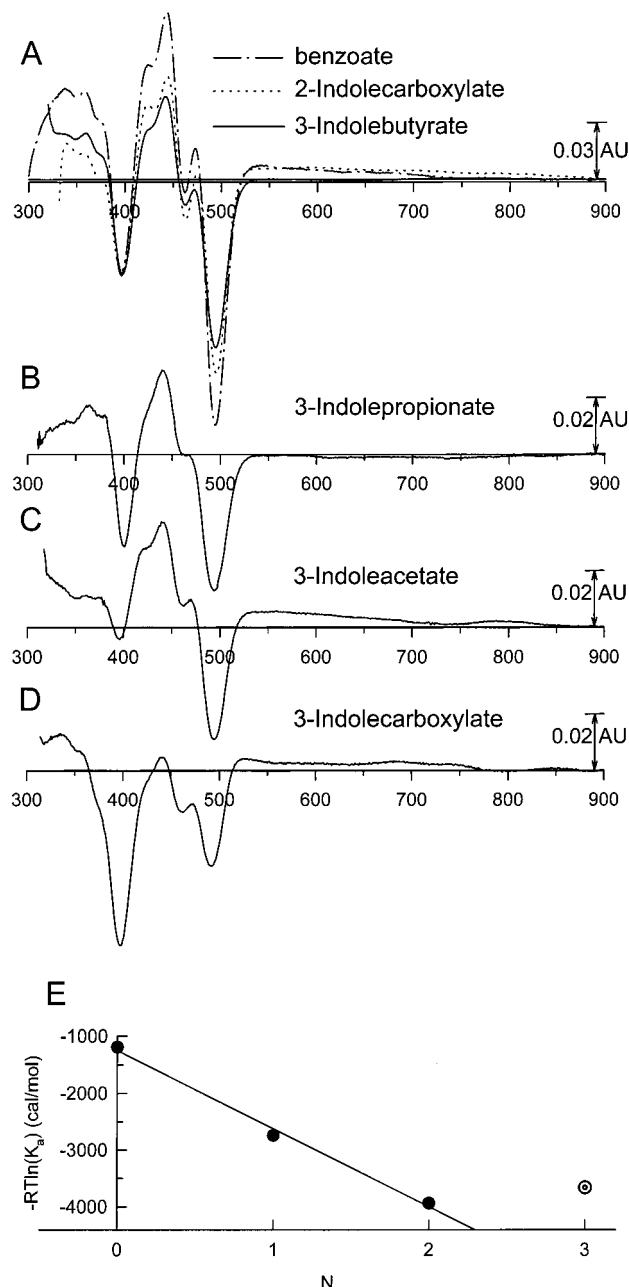


FIGURE 5: Comparison of difference spectra obtained for complexes formed with MTOX and various aromatic carboxylic acid derivatives (panels A–D). Spectra were normalized to the same initial concentration of uncomplexed MTOX ($A_{457} = 0.5$, 37.6 μ M MTOX) and to 100% complex formation, as described in Experimental Procedures. Panel E: The energy of complex formation with MTOX and 3-indole-(CH₂)_{*n*}-CO₂⁻ is plotted as a function of n . The data obtained when $n = 3$ (dotted circle) was not included in the linear regression fit shown by the solid line.

doleacrylate ($K_d = 5.5$ mM). Addition of a polar hydroxyl group that might act as a hydrogen bond acceptor or donor results in a nearly 3-fold increase in binding affinity, as shown by studies with 3-indolelactate ($K_d = 0.28$ mM). MSOX ligands containing a hydrogen bond donor at an equivalent position relative to the carboxyl group (R-CH-(XH)-CO₂⁻) form a hydrogen bond with the backbone carbonyl of gly344, a residue that is conserved in MTOX (gly337) (10, 11).

In the case where the carboxylate is directly attached to the indole ring (indole-(CH₂)_{*n*}-CO₂⁻, $n = 0$), shifting the

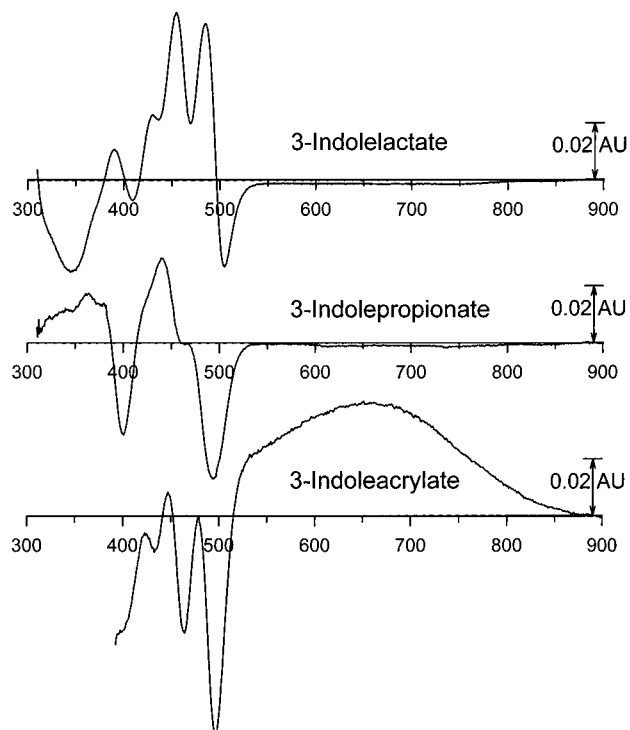


FIGURE 6: Comparison of difference spectra obtained for complexes of MTOX with various 3-indolepropionate derivatives. Spectra are normalized as described in the legend to Figure 5.

substituent from the 3 to the 2 position resulted in a surprising 6-fold increase in binding affinity ($K_d = 115$ versus 18.3 mM). This suggests that 2-indolecarboxylate might adopt an alternate binding mode that is not accessible by 3-indolecarboxylate. The dissociation constant observed for 2-indolecarboxylate is within the same range obtained with other aromatic carboxylates, including benzoate ($K_d = 37.2$ mM), anthranilate ($K_d = 11.8$ mM), and pyrrole-2-carboxylate ($K_d = 25.1$ mM).

Qualitatively similar spectral perturbations are observed with 3-indole-(CH₂)_n-CO₂⁻ ($n = 0$ to 3), 2-indole-CO₂⁻, and benzoate, as judged by difference spectra that exhibit negative peaks around 500 and 400 nm and positive peaks around 450 and 350 nm (Figure 5, panels A–D). However, differences in the magnitude of the perturbation are observed within this group; in particular, benzoate, 2-indolecarboxylate, and 3-indolebutyrate elicit perturbations that are significantly larger than those seen with the other ligands. Qualitatively different perturbations are observed when a hydroxyl group or a double bond is introduced into the side chain of indole-3-propionate (Figure 6), especially in the latter case where a charge-transfer complex is formed with MTOX and 3-indoleacrylate ($\lambda_{\max} = 650$ nm). Charge-transfer complexes are also formed with pyrrole-2-carboxylate ($\lambda_{\max} = 530$ nm) and anthranilate where a broad and weak band is seen in the long wavelength region (data not shown). The magnitude of the perturbation with anthranilate was significantly smaller than all other ligands tested, exactly opposite to that observed with benzoate.

Sarcosine Analogues as Ligands. Since sarcosine is oxidized by MTOX, various analogues were tested as possible substrates or inhibitors (Table 3). MTOX exhibits similar binding affinity for sarcosine and *N,N'*-dimethylglycine, while the complex formed with *N*-benzylglycine is

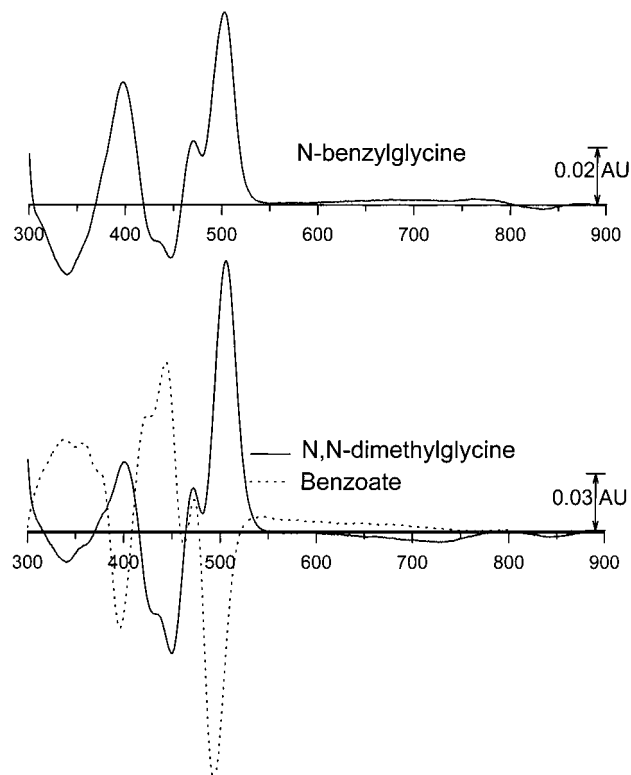


FIGURE 7: Comparison of difference spectra obtained for MTOX complexes with two glycine derivatives and benzoate. Spectra are normalized as described in the legend to Figure 5.

5-fold more stable. Neither *N,N'*-dimethylglycine nor *N*-benzylglycine acts as a substrate for MTOX. The results with *N,N'*-dimethylglycine suggest that MTOX is specific for secondary amines, as observed with MSOX (6). Qualitatively similar spectral perturbations are observed with both sarcosine analogues. The magnitude of the perturbation is greater with *N,N'*-dimethylglycine and on a par with that observed with benzoate (Figure 7). Interestingly, difference spectra observed for the MTOX complexes with *N,N'*-dimethylglycine and *N*-benzylglycine are virtually mirror images of that observed with benzoate and 3- or 2-substituted indole alkyl carboxylates. This difference arises because the sarcosine analogues cause bathochromic shifts of the 457 and 382 nm bands of free MTOX (e.g., to 464 and 387 nm, respectively, with *N,N'*-dimethylglycine), whereas hypsochromic shifts are observed with benzoate and the indole derivatives.

Charge-transfer complexes are formed with MTOX and sarcosine analogues (CH₃XCH₂CO₂⁻), where the amino group is replaced by various group VI elements (X = S, Se, or Te), as evidenced by the appearance of new absorption bands at longer wavelengths (Figure 8). The charge-transfer band when X = S is not well-resolved in the absolute spectrum owing to overlap with the red edge of the flavin absorption spectrum. This band position was estimated from difference spectra (not shown). The energy of the charge-transfer bands varied, depending on the nature of X (S > Se > Te) ($\lambda_{\max} = 516, 561, \text{ and } 652$ nm, respectively). In these complexes, the electron-deficient flavin is likely to act as charge-transfer acceptor. The energy of the charge-transfer bands should therefore be correlated with the 1-electron reduction potentials of the donor ligands. Indeed, an excellent linear correlation ($r^2 = 0.998$) is observed between charge-

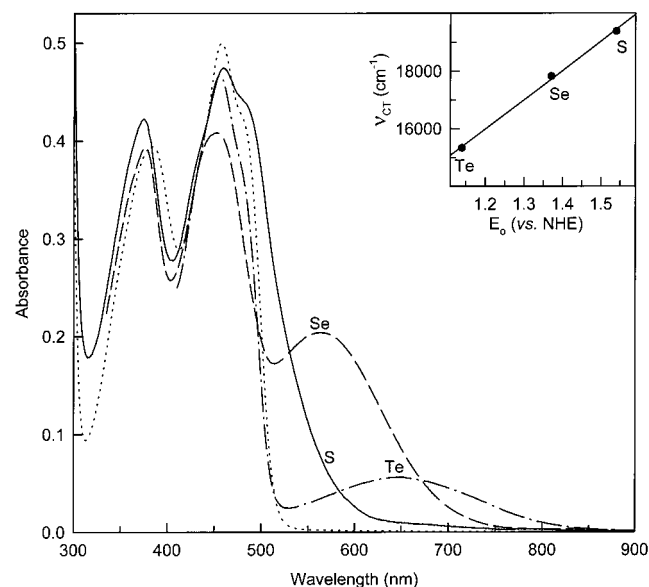
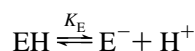
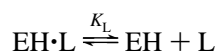


FIGURE 8: Charge-transfer complexes formed with MTOX and $\text{CH}_3\text{XCH}_2\text{CO}_2^-$. The absorption spectrum of free MTOX (dotted line) is compared with the complexes formed when $\text{X} = \text{S}$ (solid line), Se (dashed line), or Te (dash-dot line). All spectra are normalized as described in the legend to Figure 5. The inset shows a plot of the energy of the charge-transfer bands versus E° values estimated for the ligands, as described in the text.

transfer band energy and the 1-electron reduction potentials of the ligands, as estimated by E° values reported for a series of diaryl chalcogenides $[(\text{C}_6\text{H}_5)_2\text{X}^{+}/(\text{C}_6\text{H}_5)_2\text{X}]$ (24) (Figure 8, inset). A similar correlation has been observed for the corresponding complexes formed with $\text{CH}_3\text{XCH}_2\text{CO}_2^-$ and MSOX (11).

Effect of pH on the Stability of the MTOX–Benzoate Complex. The binding affinity of benzoate ($\text{pK}_a = 4.17$) increased by 2 orders of magnitude when the pH was decreased from 9 to 5.7 (Figure 9). Analysis of the data according to the rules of Dixon (25) indicates that benzoate binding is enhanced upon protonation of a group in enzyme–benzoate complex ($\text{pK}_{\text{EL}} = 6.87$).



$$-\log K_{\text{d obs}} = -\log K_{\text{L}} - \log(1 + K_{\text{E}}/[\text{H}^+]) + \log(1 + [\text{H}^+]/K_{\text{EL}}) \quad (4)$$

Benzoate binding is also affected by a group in the free enzyme or ligand. This group is assigned to the free enzyme on the basis of the estimated pK_a ($\text{pK}_{\text{E}} = 8.41$). Ionization of this group appears to prevent benzoate binding to MTOX.

DISCUSSION

These studies provide the first evidence that *solA* is actually a functional gene in *E. coli*, as judged by the observed expression in a wild-type *E. coli* K-12 strain. Expression levels are enhanced about 3-fold by growth on minimal as compared with rich media. Unlike the sarcosine-

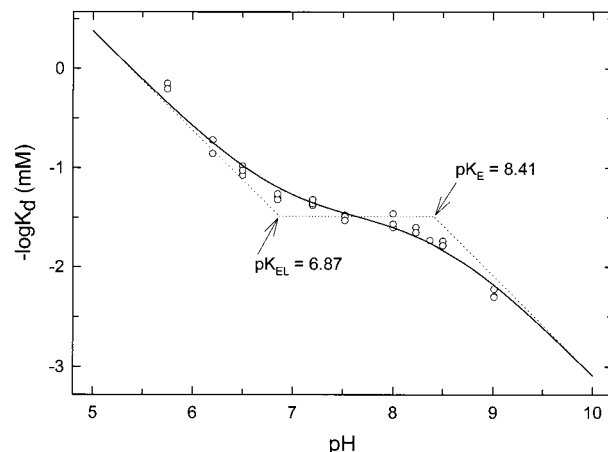


FIGURE 9: Effect of pH on benzoate binding to MTOX. The solid curve is the fit of the data to eq 4 ($\text{pK}_{\text{E}} = 8.41$, $\text{pK}_{\text{EL}} = 6.87$, $K_{\text{E}} = 31 \text{ mM}$). The dotted lines have slopes equal to 0 or -1 .

inducible bacterial sarcosine oxidases, MTOX expression in cells grown on minimal media is not affected by *N*-methyl-L-tryptophan. MTOX expression is also unaffected by indoleacrylate, a compound that induces expression of tryptophan biosynthesis genes that are under the control of the *trp* promoter (18, 19). Studies to determine the effect of a *solA* gene knockout on cell viability and expression of other genes may provide insight regarding the physiological role of MTOX in *E. coli*.

Recombinant MTOX forms an anionic flavin semiquinone and a reversible, covalent flavin–sulfite complex, properties characteristic of flavoprotein oxidases. Mutagenesis and structural studies with lactate oxidase suggest that these reactions, which result in the development of negative charge at the N(1)–C(2)–O locus of the flavin ring, are facilitated by a nearby positive charge on the protein (26). Lys341 is likely to serve as the positively charged group in MTOX since it aligns with lys348 in MSOX; the ϵ -amino group of lys348 in MSOX forms a hydrogen bond with the flavin C(2) carbonyl oxygen in MSOX (10).

The extremely slow rate of sulfite complex formation observed with MTOX is very atypical in comparison with most other flavoprotein oxidases. A very slow reaction with sulfite has, however, been observed with MSOX (11), suggesting that there may be a significant kinetic barrier against sulfite complex formation with MTOX and its homologues. Dissociation (K_{d}) and rate constants (k_{on}) reported for sulfite complex formation with other flavoprotein oxidases (27–30) and free FAD (31) vary by more than 6 orders of magnitude. An apparently linear relationship is observed when $\log k_{\text{on}}$ is plotted versus $\log K_{\text{d}}$ ($r^2 = 0.90$, slope = -0.95) (Figure 10, panel A). This result can be explained by the fact that the observed variation in K_{d} is largely due to differences in k_{on} since the complexes exhibit surprisingly similar values for the rate of complex dissociation (k_{off}) (Figure 10, panel B). In comparison, the MTOX–sulfite complex would appear to be about 3 orders of magnitude more stable than expected based on the slow rate of complex formation. The anomalous stability of the MTOX–sulfite complex can be explained by the fact that the rate of complex dissociation is about 3 orders of magnitude slower than observed for the other complexes (Figure 10, panel B) and therefore counterbalances the effect of the slow rate of complex formation.

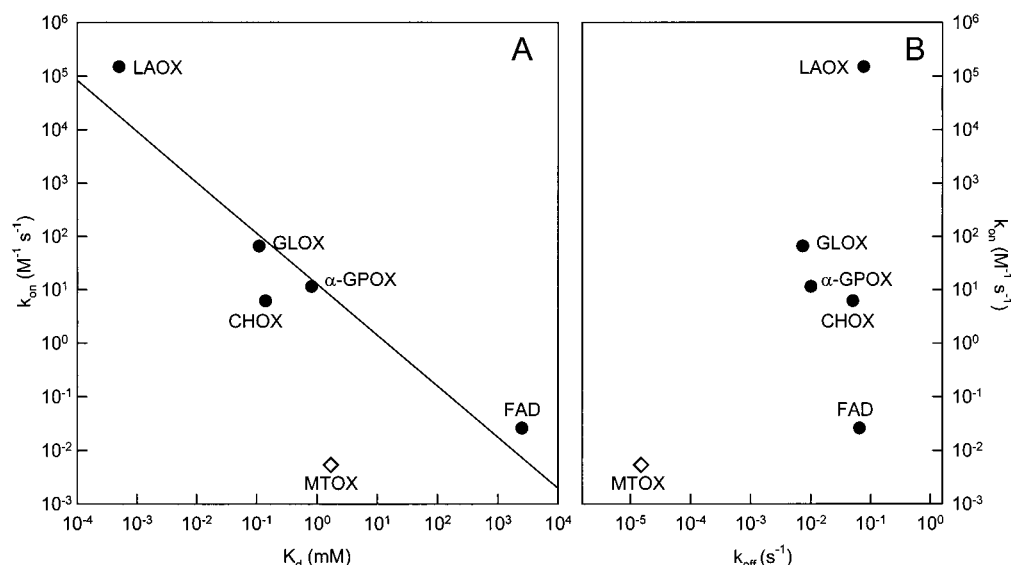


FIGURE 10: The correlation between dissociation constants for various flavin–sulfite complexes and the rates of complex formation is shown in panel A. Rates of complex formation are plotted versus rates of complex dissociation in panel B. Solid circles show data reported for lactate oxidase (LAOX) (25 °C, pH 7) (30), glucose oxidase (GLOX) (25 °C, pH 5.6) (29), cholesterol oxidase (CHOX) (25 °C, pH 7) (28), α -glycerophosphate oxidase (α -GPOX) (25 °C, pH 7) (27), and free FAD (25 °C, pH 7) (31). The data obtained with MTOX (open diamond) was not included in the linear regression fit shown by the solid line in panel A.

The pK_a for ionization at N(3)H of FAD attached to MTOX (8.36) is two pH units lower than observed for free FAD (10.4) (23). A decreased pK_a value for N(3)H ionization is not a universal feature but has been observed with a number of other flavoprotein oxidases (MSOX, glycolate oxidase, nitroalkane oxidase, long-chain 2-hydroxy acid oxidase, and α -glycerophosphate oxidase) that exhibit pK_a values in the range from 6.4 to 8.5 (11, 32–36). Mutagenesis studies with glycolate oxidase suggest that the anionic oxidized flavin may be stabilized by hydrogen bonding between the C(4) carbonyl oxygen of the flavin and the hydroxyl group of an active site tyrosine (tyr129) (37). Other factors must also play a role since hydrogen bonding to the C(4) carbonyl oxygen is observed with many flavoenzymes, most of which do not exhibit a low pK_a for N(3)H ionization. Indeed, the ability of the flavin ring to form hydrogen bonds appears to be fully satisfied in flavoenzymes, as judged by a recent survey of a diverse group of known structures (38).

In these studies, we have identified a number of active site ligands that have proved useful in probing the kinetic mechanism of *N*-methyltryptophan oxidation (2) and in ongoing crystallographic studies. The MTOX ligands include aromatic carboxylates [benzoate, 3-indole-(CH₂)_{*n*}-CO₂[−] (*n* = 0 to 3), 2-indole-CO₂[−]] that act as competitive inhibitors with respect to *N*-methyl-L-tryptophan and elicit qualitatively similar perturbations of the visible absorption spectrum of the enzyme. Significantly, the tightest binding with 3-substituted indole carboxylates is observed with 3-indolepropionate [3-indole-(CH₂)₂-CO₂[−] K_d = 0.79 mM], a derivative where the side chain length is the same as the best known substrate, *N*-methyltryptophan. The analysis of the binding data for 3-substituted indole carboxylates shown in Figure 5, panel E suggests that each methylene group contributes about 1.4 kcal/mol to binding energy. In this case, the two methylene groups in 3-indolepropionate would provide 70% of the observed binding energy with only 1250 cal/mol attributable to the combined contribution of the carboxyl group and the indole ring. The carboxyl group is expected

to form hydrogen bonds with lys341 and arg51, as judged by the interactions observed for the ligand carboxylate in various MSOX–inhibitor complexes (10, 11). Since these interactions should contribute about 1–2 kcal/mol to the binding energy, the analysis would suggest that the indole moiety in 3-indolepropionate and *N*-methyl-L-tryptophan does not contribute significantly to binding energy. This conclusion cannot, however, be correct since it predicts similar binding affinity for propionate and 3-indolepropionate; in fact, propionate is a very poor ligand for MTOX (K_d > 500 mM).²

The effect of pH on the stability of the MTOX–benzoate complex indicates that binding is enhanced upon protonation of a group in the enzyme–benzoate complex (pK_{EL} = 6.87) but blocked by ionization of a group in the free enzyme (pK_E = 8.41). Two factors suggest that the ionizable group in the free enzyme is the N(3)H position of FAD: (i) The pK_a observed for N(3)H ionization (pK_a = 8.36) is very similar to the value obtained for pK_E ; (ii) The N(3)H position of FAD is likely to be close to the negatively charged ligand carboxylate in the MTOX–benzoate complex and exert considerable electrostatic repulsion upon ionization, as judged by the structure of the MSOX–pyrrole-2-carboxylate complex where the ligand carboxylate oxygens are 3.5 Å from flavin N(3) (10, 11). The identity of the ionizable group in the MTOX–benzoate complex is less clear. Several candidates are, however, suggested based on the structure of the MSOX–pyrrole-2-carboxylate complex where the ligand carboxylate forms hydrogen bonds with the side chains of lys348 and arg52 (lys341 and arg 51 in MTOX) and is less than 4.5 Å from the ionizable groups of tyr55 and glu57 (tyr54 and glu56, respectively, in MTOX).

The sarcosine analogues, *N,N'*-dimethylglycine and *N*-benzylglycine, also bind to the active site of MTOX and elicit similar spectral perturbations. Intriguingly, difference spectra

² P. Khanna and M. S. Jorns, unpublished results.

³ P. Trickey and M. S. Jorns, unpublished results.

observed for the complexes with *N,N'*-dimethylglycine and *N*-benzylglycine are virtually mirror images of that observed with aromatic carboxylates such as benzoate, 3-indole-(CH₂)_{*n*}-CO₂[−] (*n* = 0 to 3), and 2-indole-CO₂[−]. Structural studies are needed to determine whether the two types of spectral perturbations may be associated with different binding modes or active site conformations, as observed with different classes of *p*-hydroxybenzoate hydroxylase–inhibitor complexes (39). Additional evidence suggesting possible alternate binding modes for MTOX ligands is provided by the surprising 6-fold increase in binding affinity observed when the carboxyl group in 3-indolecarboxylate is shifted to the 2 position.

In these studies, we have observed several notable similarities between MTOX and MSOX with respect to the properties of the flavin and its environment. In addition to low *pK_a* values for flavin N(3)H ionization and an apparent kinetic barrier against sulfite complex formation, a number of compounds (e.g., benzoate, pyrrole-2-carboxylate, and *N,N'*-dimethylglycine) are found to act as ligands for both MTOX and MSOX (11) with binding constants that differ by a factor of about 10 or less. Both enzymes form a series of charge-transfer complexes with CH₃XCH₂CO₂[−], (X = S, Se, Te). In each case, an excellent correlation is found between the energy of the charge transfer bands and the 1-electron reduction potentials of the ligands. The results are consistent with the observed sequence homology and conservation of many active site residues, suggesting that the enzymes will exhibit significant structural similarity. Despite these similarities, the two enzymes exhibit dramatic differences in substrate specificity and are likely to have different physiological functions, as evidenced, in part, by the fact that MTOX is constitutive enzyme in *E. coli* whereas MSOX expression in various bacteria is induced by sarcosine. *N*-Methyl-L-tryptophan is not oxidized by MSOX. The turnover rate of MTOX with sarcosine is 0.54% of that observed with *N*-methyl-L-tryptophan (2) and 0.35% of the turnover rate of MSOX with sarcosine (6). Steric interference was observed when an attempt was made to model a tryptophan side chain into the MSOX active site.³ The MTOX active site must clearly be considerably larger to accommodate the bulky side chains of its preferred substrates. The key role of bulky side chains in the preferred MTOX substrates may be to promote the proper positioning of the substrate in the active site. The slow turnover of MTOX with sarcosine may reflect the fact that the small substrate may adopt many alternate conformations in the larger MTOX active site, only a small fraction of which may constitute productive complexes (40).

ACKNOWLEDGMENT

We thank Dr. Louis Silks [National Stable Isotope Resource at Los Alamos and NIH Supported Resource (RR02231)] for his generous gifts of methylselenoacetate and methyltelluroacetate. We also thank Dr. Paul Fitzpatrick for helpful discussions.

REFERENCES

- Koyama, Y., and Ohmori, H. (1996) *Gene* 181, 179–183.
- Khanna, P., and Jorns, M. S. (2001) *Biochemistry* 40, 1451–1459.
- Kvalnes-Krick, K., and Jorns, M. S. (1991) in *Chemistry and Biochemistry of Flavoenzymes* (Muller, F., Ed.) pp 425–435, CRC Press, Inc., Boca Raton, FL.
- Cannon, J. R., and Williams, J. R. (1982) *Aust. J. Chem.* 35, 1497–1500.
- Jansen, R., Kunze, B., Reichenbach, H., and Hoefle, G. (1996) *Liebigs Ann. Org. Bioorg. Chem.* 2, 285–290.
- Wagner, M. A., and Jorns, M. S. (2000) *Biochemistry* 39, 8825–8829.
- Wagner, M. A., Khanna, P., and Jorns, M. S. (1999) *Biochemistry* 38, 5588–5595.
- Chlumsky, L. J., Zhang, L., and Jorns, M. S. (1995) *J. Biol. Chem.* 270, 18252–18259.
- Reuber, B. E., Karl, C., Reimann, S. A., Mihalik, S. J., and Dodt, G. (1997) *J. Biol. Chem.* 272, 6766–6776.
- Trickey, P., Wagner, M. A., Jorns, M. S., and Mathews, F. S. (1999) *Structure* 7, 331–345.
- Wagner, M. A., Trickey, P., Chen, Z., Mathews, F. S., and Jorns, M. S. (2000) *Biochemistry* 39, 8813–8824.
- Ashton, W. T., Brown, R., Jacobson, F., and Walsh, C. (1979) *J. Am. Chem. Soc.* 101, 4419–4420.
- Ausubel, F. M., Brent, R., Kingston, R. E., Moore, D. D., Seidmen, J. G., Smith, J. A., and Struhl, K. (1989) in *Current Protocols in Molecular Biology*, John Wiley and Sons, New York.
- Moore, J. T., Uppal, A., Maley, F., and Maley, G. F. (1993) *Protein Expression Purif.* 4, 160–163.
- Vogel, H. J., and Bonner, D. M. (1956) *J. Biol. Chem.* 218, 97–106.
- Jensen, K. A. (1993) *J. Bacteriol.* 175, 3401–3407.
- Kvalnes-Krick, K., and Jorns, M. S. (1986) *Biochemistry* 25, 6061–6069.
- Border, K. L., Beckman, P., and Lane, A. N. (1991) *Eur. J. Biochem.* 202, 459–470.
- Czernik, P. J., Shin, D. S., and Hurley, J. K. (1994) *J. Biol. Chem.* 269, 27869–27875.
- Massey, V., Muller, F., Feldberg, R., Schuman, M., Sullivan, P. A., Howell, L. G., Mayhew, S. G., Matthews, R. G., and Foust, G. P. (1969) *J. Biol. Chem.* 244, 3999–4006.
- Massey, V., and Palmer, G. (1966) *Biochemistry* 5, 3181–3189.
- Massey, V., and Hemmerich, P. (1978) *Biochemistry* 17, 9–17.
- Massey, V., and Ganther, H. (1965) *Biochemistry* 4, 1161–1173.
- Engman, L., Lind, J., and Merenyi, G. (1994) *J. Phys. Chem.* 98, 3174–3182.
- Dixon, M., and Webb, E. C. (1979) *Enzymes*, pp 138–164, Academic Press, New York.
- Muh, U., Massey, V., and Williams, C. H. (1994) *J. Biol. Chem.* 269, 7982–7988.
- Parsonage, D., Luba, J., Mallett, T. C., and Claiborne, A. (1998) *J. Biol. Chem.* 273, 23812–23822.
- Gadda, G., Wels, G., Pollegioni, L., Zucchelli, S., Ambrosius, D., Pilone, M. S., and Ghisla, S. (1997) *Eur. J. Biochem.* 250, 369–376.
- Frederick, K. R., Tung, J., Emerick, R. S., Masiarz, F. R., Chamberlain, S. H., Vasavada, A., Rosenberg, S., Chakraborty, S., Schopfer, L. M., and Massey, V. (1990) *J. Biol. Chem.* 265, 3793–3802.
- Maedayorita, K., Aki, K., Sagai, H., Misaki, H., and Massey, V. (1995) *Biochimie* 77, 631–642.
- Muller, F., and Massey, V. (1969) *J. Biol. Chem.* 244, 4007–4016.
- Schuman, M., and Massey, V. (1972) *Biochim. Biophys. Acta* 227, 500–520.
- Macheroux, P., Massey, V., Thiele, D. J., and Volokita, M. (1991) *Biochemistry* 30, 4612–4619.
- Gadda, G., and Fitzpatrick, P. F. (1998) *Biochemistry* 37, 6154–6164.
- Belmouden, A., and Lederer, F. (1996) *Eur. J. Biochem.* 238, 790–798.
- Claiborne, A. (1986) *J. Biol. Chem.* 261, 14398–14407.

37. Macheroux, P., Kieweg, V., Massey, V., Soderlind, E., Stenberg, K., and Lindqvist, Y. (1993) *Eur. J. Biochem.* 213, 1047–1054.
38. Fraaije, M. W., and Mattevi, A. (2000) *Trends Biol. Sci.* 25, 126–132.
39. Gatti, D. L., Palfey, B. A., Lah, M. S., Entsch, B., Massey, V., Ballou, D. P., and Ludwig, M. L. (1994) *Science* 266, 110–114.
40. Bruice, T. C., and Benkovic, S. J. (2000) *Biochemistry* 39, 6267–6274.

BI0024411